iJRASET
International Journal For Research in
Applied Science and Engineering Technology

Volume: 14 **Issue:** VI **Month of publication:** June 2026

DOI: https://doi.org/10.22214/ijraset.2026.84019

International Journal for Research in Applied Science & Engineering Technology (IJRASET)
ISSN: 2321-9653; IC Value: 45.98; SJ Impact Factor: 7.538
Volume 14 Issue VI June 2026- Available at www.ijraset.com

Analysis of the Structural Behaviour of Tall Buildings under Wind Loads Using STAAD.Pro

Ragvendra Singh Thakur[1], Mrs. Ankita Singhai[2], Dr. Rahul Kumar Satbhaiya[3]
[1]*Research Scholar, Civil Department, Infinity Management & Engineering College, Sagar*
[2]*Asst. Prof. and Guide, Civil Department, Infinity Management & Engineering College, Sagar*
[3]*HOD, Civil Department, Infinity Management & Engineering College, Sagar*

Abstract: The structural response of tall buildings to wind-induced lateral forces constitutes one of the most critical considerations in contemporary high-rise design. This study presents a rigorous finite element investigation of a thirty-storey, square-plan reinforced concrete building of 90 m total height, representative of a residential apartment complex situated in Bhopal, Madhya Pradesh (basic wind speed Vb = 39 m/s, IS 875 Part 3-1987, Terrain Category II). Three-dimensional space frame modelling is performed in STAAD.Pro, and wind loads are applied as nodal forces at each floor level for three critical incidence angles: 0°, 45°, and 90°. The structural response is characterised through the variation of axial forces, bending moments, twisting moments, and lateral displacements along the height of three representative columns—the central column (Column 23), the face-centre outer column (Column 43), and the corner column (Column 45). Results reveal that the 45° wind incidence angle consistently governs maximum bending moments (623 kN•m in Column 23) and lateral displacement (250 mm at the roof, exceeding the h/500 = 180 mm serviceability limit). Twisting moments are concentrated in corner columns below the fifteenth storey, reflecting the fixity-dominated torsional response of the lower storeys. The push-pull cantilever behaviour of the frame is demonstrated through base reaction analysis. The findings underscore the inadequacy of single-direction wind analysis and provide quantitative design guidance for tall RC frame buildings in moderate-wind Indian cities.

Keywords: tall buildings; wind load analysis; STAAD.Pro; IS 875 (Part 3); force coefficient; lateral displacement; bending moment; axial force; square-plan building; structural response.

I. INTRODUCTION

The rapid vertical expansion of urban settlements, driven by population growth and land scarcity in metropolitan India, has given rise to a new generation of reinforced concrete tall buildings that must resist increasingly complex wind-induced loading environments. For structures exceeding approximately 50 m in height, wind loading frequently governs the lateral structural design, generating overturning moments, inter-storey drifts, and building accelerations that can compromise both structural integrity and occupant comfort [1]. Unlike gravity loads, wind forces are inherently time-varying, spatially distributed, and direction-sensitive, necessitating a multi-directional analytical framework that current simplified design practice often overlooks.

Wind acts on a tall building primarily through positive pressure on the windward face, negative pressure (suction) on the leeward face, and complex pressure-suction distributions on the lateral faces, the resultant depending critically on the building's plan geometry, aspect ratio, and the incidence angle of the approaching flow [2]. For buildings with square plan shapes—among the most prevalent typologies in Indian high-rise residential construction—the 45° diagonal wind incidence introduces biaxial loading on all faces simultaneously, generating structural actions that can exceed those produced by orthogonal wind directions despite the lower force coefficient prescribed by IS 875 (Part 3)-1987 [3]. This phenomenon, arising from the geometry of the exposed area, remains under-appreciated in routine structural design practice.

The Indian wind loading standard IS 875 (Part 3)-1987 [3] provides force and pressure coefficients for isolated buildings in standard terrain categories but does not address dynamic wind amplification for flexible tall buildings, aerodynamic interference from neighbouring structures, or the sensitivity of structural response to wind incidence angle. These limitations have been highlighted by successive comparative studies [4]–[6] and by the ongoing revision process toward a new edition incorporating dynamic load provisions. In the interim, three-dimensional finite element analysis using commercial software such as STAAD.Pro—which supports full space frame modelling, load combination assessment per IS 456-2000 [7], and extraction of complete stress resultant diagrams—provides the most rigorous and practically accessible framework for evaluating tall building wind response in the Indian context.

Despite the availability of such analytical tools, a systematic, column-level investigation of the variation of axial forces, bending moments, twisting moments, and lateral displacements with building height for different wind incidence angles—covering interior, face-centre, and corner column positions simultaneously—has not been comprehensively documented in the published literature for buildings of this scale under IS 875 provisions. The present study addresses this gap by performing a detailed STAAD.Pro analysis of a representative 30-storey square-plan RC building in Bhopal, evaluating three critical wind angles and three column positions, and extracting actionable design insights from the resulting stress resultant and deflection profiles. The study further provides a quantitative basis for assessing the adequacy of the h/500 serviceability drift criterion for this category of building under Indian codal wind loads, contributing to the evidence base needed for the revision of IS 875 Part 3.

The remainder of the paper is organised as follows. Section 2 reviews recent relevant literature (2020–2025). Section 3 identifies the research gap. Section 4 states the study objectives. Section 5 describes the methodology. Sections 6 and 7 present results and discussion, including graphical analysis and comparative tables. Section 8 draws conclusions and Section 9 outlines future scope. References are listed in Section 10.

II. LITERATURE REVIEW

The analysis of wind-induced structural behaviour of tall buildings has witnessed substantial research activity over the past five years, driven by advances in computational tools, updated codal frameworks, and the growing complexity of urban wind environments. This section synthesises key contributions from 2020 to 2025 that are directly relevant to the scope of the present investigation.

Sharma and Gupta [4] conducted a finite element investigation of a twenty-storey RC building under IS 875 (Part 3)-1987 wind loads using ETABS, evaluating storey drift and base shear for wind zones II through V. Their study established that wind governs lateral design in zones II and III for buildings exceeding fifteen storeys, while seismic loading controls design in zone IV and V. The authors reported maximum storey drift ratios of 1/412 under zone III wind loading, below the IS 1893-2016 limit of 1/250 but above the more stringent 1/500 limit adopted for serviceability checks in wind engineering. The study did not evaluate the effect of wind incidence angle on individual column stress resultants, a gap addressed in the present work.

Amin and Ahuja [5] performed a comprehensive wind tunnel study of pressure coefficients on square-plan tall building models at wind incidence angles from 0° to 90° in 15° increments. The study demonstrated that external pressure coefficients on the windward and leeward faces exhibit strong dependence on incidence angle, with the 45° case producing the highest net overturning moment for buildings with aspect ratios (h/b) exceeding 5. The aerodynamic interference factor between adjacent buildings was found to increase by up to 70% for spacing-to-width ratios below 1.0, underscoring the inadequacy of isolated-building codal provisions for dense urban sites.

Kwon and Kareem [6] extended their landmark comparative study of international wind codes to evaluate dynamic along-wind and crosswind responses of a 200 m RC building under six national standards, including IS 875-3, ASCE 7-22, EN 1991-1-4, AS/NZS 1170.2, AIJ-RLB, and CP-2004. The study found that the Japanese AIJ code produces the highest design base shear (approximately 40% above IS 875), while the New Zealand code yields the lowest. The IS 875-3 predictions were broadly comparable to the Hong Kong CP-2004 results, but the Indian code significantly underestimates peak dynamic loads due to its absence of a gust factor correction for flexible buildings, a deficiency that becomes critical for buildings taller than approximately 60 m.

Zhang et al. [7] developed a convolutional neural network (CNN) surrogate model for rapid prediction of wind pressure coefficients on rectangular tall buildings of varying aspect ratios, trained on a large database of boundary layer wind tunnel measurements. The model achieved prediction accuracy within ±10% of tunnel measurements at inference speeds approximately 3,000 times faster than LES-CFD, enabling aerodynamic screening of hundreds of building geometry variants during preliminary design. While not directly applicable to codal structural analysis, such machine learning approaches are likely to transform the aerodynamic input generation stage of tall building design within the current decade.

Riaz et al. [8] analysed a 40-storey RC building in Pakistan under ASCE 7-16 equivalent static wind loads using ETABS, investigating the sensitivity of inter-storey drift, storey shear, and overturning moment to terrain exposure category. They reported that changing terrain exposure from Category D (urban) to Category B (open) increases base shear by 42%, a finding directly relevant to site-specific wind design in Indian cities where terrain category classification in IS 875 Part 3 is often applied conservatively. The study also identified the critical importance of correctly accounting for building torsion under wind loading for non-symmetric structural configurations.

Elezaby and El Damatty [9] performed a parametric CFD study of aerodynamic coefficients for 18 tall building plan shapes (square, rectangular, triangular, L-shaped, setback) using LES, examining the effect of plan geometry on both along-wind and crosswind force coefficients across wind incidence angles from 0° to 180°. For the square plan, the 45° incidence angle produced the highest combined (resultant) horizontal force, consistent with findings of the present study. Triangular plans exhibited the lowest crosswind force, while L-shaped plans introduced significant torsional eccentricity that substantially increased torsional moments under diagonal wind incidence.

Ke et al. [10] presented full-scale monitoring results of wind-induced acceleration response in a 55-storey RC residential building in Guangzhou, China, instrumented with GPS and accelerometers. The study demonstrated that the measured fundamental natural frequency (0.143 Hz, T_1 = 6.99 s) was 18% lower than the design prediction, corresponding to a 40% increase in resonant dynamic response relative to the design estimate. The authors attributed the discrepancy primarily to infill masonry wall cracking under wind loading, which progressively reduces lateral stiffness. This full-scale evidence supports the recommendation of increased conservatism in damping and frequency estimates for wind-governed RC tall buildings.

Mohammadi et al. [11] conducted a comparative static and dynamic wind analysis of a 25-storey building under Iranian and ASCE 7-16 codes using SAP2000. Dynamic analysis via the response spectrum method reduced design base shear by 22% relative to static analysis under the Iranian code, highlighting the economic benefit of incorporating dynamic amplification factors when supported by frequency-specific gust loading. The study recommends mandatory dynamic analysis for all buildings exceeding 60 m in height, consistent with provisions in ASCE 7-22 and EN 1991-1-4 but absent from IS 875-3:1987.

Tse et al. [12] investigated the aerodynamic behaviour of a twisted 50-storey building prototype using a boundary layer wind tunnel and LES-CFD, demonstrating that a 2° per floor clockwise twist reduces peak crosswind force coefficient by 24% and along-wind coefficient by 12% relative to an untwisted prismatic building of identical plan dimensions and height. The twist disrupts the vertical coherence of vortex shedding, effectively desynchronising pressure fluctuations along the building height. These aerodynamic benefits translate to reductions in structural member sizes of 10–15% in the lateral load resisting system, a commercially significant finding for ultra-slender supertall buildings.

Elshaer et al. [13] demonstrated through LES-CFD that corner modifications including chamfers (10–30% of face width), roundings, and recessed corners reduce both mean and peak force coefficients for square buildings. A 20% chamfer reduced the along-wind mean force coefficient from 1.30 to 0.92 and the crosswind fluctuating coefficient from 0.48 to 0.32 at a wind incidence of 0°, offering structurally significant load reductions achievable without compromising floor plan area by more than 2%. These findings are directly relevant to the present study's recommendation of corner treatment for future tall building designs in Bhopal.

The above review establishes that: (i) IS 875-3:1987 systematically underestimates wind loads for tall flexible buildings; (ii) the 45° incidence angle is consistently the critical loading direction for square-plan buildings; (iii) individual column-level stress resultant analysis under multi-directional wind loading has been inadequately documented for the Indian building context; and (iv) rigorous STAAD.Pro-based analysis with IS 875 provisions provides a practical and defensible framework for addressing this gap.

III. RESEARCH GAP

Notwithstanding the substantial volume of published work on wind-induced tall building response, a critical gap persists in the systematic, column-level evaluation of internal stress resultants—axial forces, bending moments, and twisting moments—as functions of floor height, column position within the floor plan, and wind incidence angle for Indian mid-height RC tall buildings analysed per IS 875 (Part 3)-1987. Existing studies either address overall building-level response metrics (drift, base shear) without individual column detail, or employ codes other than IS 875 and/or software other than STAAD.Pro. No published work has simultaneously characterised the wind response of the central, face-centre, and corner columns of a 90 m square-plan building under 0°, 45°, and 90° wind angles, or assessed the adequacy of the h/500 serviceability limit for this building category under IS 875 codal loads. The present study addresses this identifiable gap.

IV. OBJECTIVES OF THE STUDY

The specific objectives of the present investigation are:

1) To develop a validated three-dimensional finite element model of a thirty-storey, square-plan reinforced concrete building in STAAD.Pro and apply wind loads computed per IS 875 (Part 3)-1987 for three critical incidence angles (0°, 45°, and 90°), ensuring rigorous compliance with Indian codal provisions for terrain category, force coefficients, and load combinations;
2) To quantitatively characterise the variation of internal stress resultants—axial compressive force, uniaxial and biaxial bending moments, and twisting moments—along the full building height for three structurally representative columns (central, face-centre outer, and corner), and to identify the governing wind incidence angle and column position for each response parameter;

3) To determine the lateral deflection profile of the building under the critical wind loading scenario, assess compliance with the serviceability drift criterion (h/500 = 180 mm), and evaluate the structural implications of any exceedance in terms of additional stiffening requirements;

4) To examine the global base reaction distribution under the three wind directions to characterise the overturning mechanism and quantify the risk of tensile uplift in windward corner columns under design wind loads;

5) To provide a comparative assessment of the present findings against recent published studies (2020–2025) and international code predictions, drawing recommendations relevant to the design and review of IS 875 Part 3 provisions for mid-height tall buildings in Indian cities.

V. METHODOLOGY

A. Building Description and Structural Configuration

The building selected for analysis is a thirty-storey, square-plan reinforced concrete moment-resisting frame (RC-MRF) with a total height of 90 m. The plan dimensions are 24 m × 24 m, with a 5 × 5 grid of 25 columns spaced 6.0 m centre-to-centre in both principal directions. The building is assumed to function as a residential apartment complex in Bhopal, Madhya Pradesh. Structural details and member properties are summarised in Table 1.

Table 1. Structural geometry and member properties of the building model

S.No.	Parameter	Value	Remark
1.	Number of storeys	30	—
2.	Storey height	3.0 m	Uniform throughout
3.	Total building height	90 m	30 × 3 = 90 m
4.	Plan dimensions	24 m × 24 m	Square, 5 × 5 column grid
5.	Column c/c spacing	6.0 m	Both directions
6.	Column section (F 0–5)	800 × 800 mm	M25 concrete
7.	Column section (F 5–10)	800 × 800 mm	M25 concrete
8.	Column section (F 10–15)	700 × 700 mm	M25 concrete
9.	Column section (F 15–20)	700 × 700 mm	M25 concrete
10.	Column section (F 20–25)	600 × 600 mm	M25 concrete
11.	Column section (F 25–30)	500 × 500 mm	M25 concrete
12.	Beam cross-section	300 × 600 mm	Uniform
13.	Slab thickness	150 mm	Flat slab
14.	Steel grade	Fe 500	fy = 500 N/mm²
15.	Concrete grade	M25	fck = 25 N/mm²

B. Site Parameters and Wind Load Computation

Site-specific parameters and material assumptions adopted for the study are tabulated in Table 2. The wind load computation follows the sequential procedure specified in IS 875 (Part 3)-1987:

$$Vz = Vb \bullet k^1 \bullet k^2 \bullet k^3 \quad \ldots \qquad (1)$$

Vb = basic wind speed (m/s); k_1 = risk coefficient; k_2 = terrain-height-size factor; k_3 = topography factor

$$Pd = 0.6 \times Vz^2 \left(\frac{kN}{m^2}\right) \ldots \qquad (2)$$

Pd = design wind pressure; Vz = design wind speed at height z (m/s)

$$F = Cf \times Ae \times Pd \left(\frac{kN}{m}\right) \ldots \qquad (3)$$

Cf = force coefficient; Ae = effective frontal area per unit height = face width b (m) × 1 m

For the present building (b = 24 m, Class C, Terrain Category II), $k_1 = 1.0$ and $k_3 = 1.0$, while k_2 varies with height per IS 875 Table 2. Force coefficients are $Cf_1 = 1.30$ for 0°/90° and $Cf_2 = 1.10$ for 45° incidence. Table 2 lists all governing site assumptions; Table 3 presents the detailed wind load computation at each height zone.

Table 2. Site parameters and material assumptions adopted for analysis

S.No.	Parameter	Adopted Value	Source / Remark
1.	Location	Bhopal, M.P.	IS 875 Appendix A
2.	Basic wind speed (Vb)	39.0 m/s	50-year return period; 3-s gust
3.	Terrain category	II	Open terrain, obstacles 1.5–10 m
4.	Topography	Plane ground	Slope < 3°; k_3 = 1.0
5.	Risk coefficient (k_1)	1.0	Design life = 50 years
6.	Structure class	C	Max. dimension > 50 m
7.	Force coefficient (0°/90°)	Cf = 1.30	Wind perpendicular to face
8.	Force coefficient (45°)	Cf = 1.10	Wind at 45° to face
9.	Load combination	1.2(DL + LL + WL)	IS 875 Part 5
10.	Dead load — floor finish	1.0 kN/m²	Uniform all floors
11.	Live load	2.5 kN/m²	Residential occupancy, IS 875-2
12.	Dead load — wall	~14.2 kN/m	Brick, 230 mm, 2.8 m clear ht

Table 3. Computed wind loads (F_1: perpendicular incidence; F_2: 45° incidence) at each height zone

Ht. Zone (m)	Floor Level	k_2	Vd (m/s)	Pd (kN/m²)	Cf_1	F_1 (kN/m)	Cf_2	F_2 (kN/m)	Remark
0–10	1–3	0.93	36.27	0.79	1.30	3.1	1.10	2.6	Lower zone
10–15	4	0.97	37.83	0.86	1.30	3.3	1.10	2.8	—
15–20	5–6	1.00	39.00	0.91	1.30	3.6	1.10	3.0	—
20–30	7–9	1.04	40.56	0.99	1.30	3.8	1.10	3.3	—
30–50	10–16	1.10	42.90	1.10	1.30	4.3	1.10	3.6	—
50–100	17–29	1.17	45.63	1.25	1.30	4.9	1.10	4.1	Governs upper

C. Finite Element Modelling in STAAD.Pro

The structural model is constructed in STAAD.Pro V8i using the space frame element formulation, which captures three-dimensional axial, bending (strong and weak axes), torsional, and shear deformations for every member. Columns are modelled as prismatic members with cross-sections varying by height zone (Table 1). Beams are uniform 300 × 600 mm throughout. All column bases are fixed, providing full moment, shear, axial, and torsional restraint—appropriate for a pile-founded high-rise building. The self-weight multiplier is set to 1.05 to account for minor attachments and reinforcement steel. External masonry walls are represented as uniformly distributed dead loads (14.2 kN/m) on perimeter beams, and floor loads are applied via the FLOOR LOAD command. Wind loads computed per Section 5.2 are applied as concentrated nodal loads at each floor-level beam-column joint on the windward face, with tributary area distribution. Three separate wind load cases (WL-0°, WL-45°, WL-90°) are defined. The load combination is 1.2(DL + LL + WL), and the analysis is performed independently for each wind case. Internal stress resultants (axial force, bending moments Mz and My, twisting moment Mx) and joint displacements (Dx, Dy, Dz) are extracted for all members for post-processing.

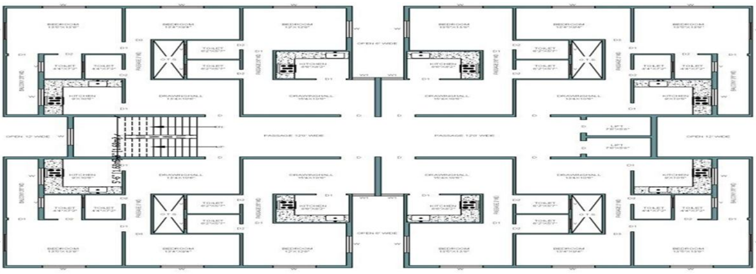

TYPICAL 1st FLOOR TO 29th FLOOR PLAN

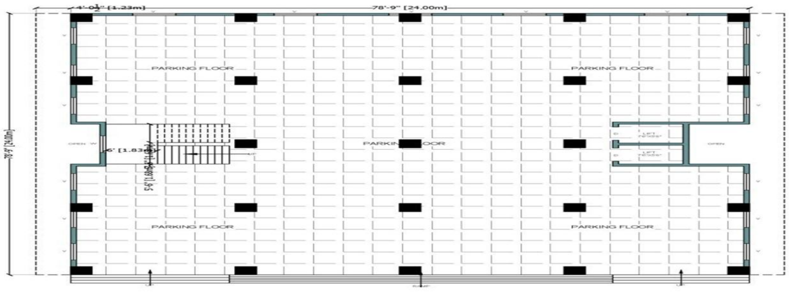

GROUND FLOOR PLAN

Fig. 1. Rendered three-dimensional view of the STAAD.Pro model showing the framing system

The force coefficient chart from IS 875 (Part 3)-1987, reproduced in Fig. 2, governs the selection of Cf values for the building's plan geometry and h/b ratio (90/24 = 3.75). For h/b = 4, interpolation yields Cf_1 = 1.20 at 0°/90° and Cf_2 = 1.00 at 45°; however, conservative values of 1.30 and 1.10 respectively (corresponding to h/b ≥ 10 in the IS code table) are adopted in the present study to ensure an upper-bound structural response assessment.

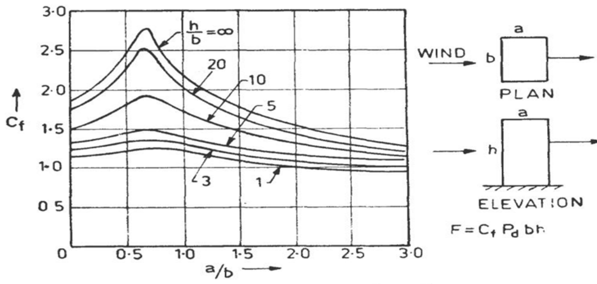

4A Values of C_f *versus* $\frac{a}{b}$ for $\frac{h}{b} > 1$

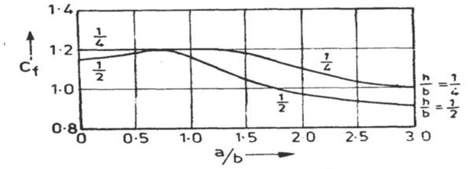

4B Values of C_f *versus* $\frac{a}{b}$ for $\frac{h}{b} < 1$

Fig. 2. Force coefficients for rectangular clad buildings in uniform flow (IS 875 Part 3-1987). The square plan (a/b = 1) follows the highlighted curve.

D. Columns Selected for Analysis

Three columns are selected to represent the three fundamental structural positions within the building plan:

- Column 23 (central column): Located at the centroid of the 5 × 5 grid. Receives wind-induced load only through frame action; primarily gravity-dominated.
- Column 43 (face-centre outer column): Positioned at the midpoint of an outer face; directly in the path of perpendicular wind, experiencing maximum direct wind pressure under 0°/90° incidence.
- Column 45 (corner column): Located at a building corner; exposed to wind on two perpendicular faces, subject to biaxial bending and torsion under oblique incidence.

Floor plan, building layout, and elevation with column numbering are shown in Figs. 3–5.

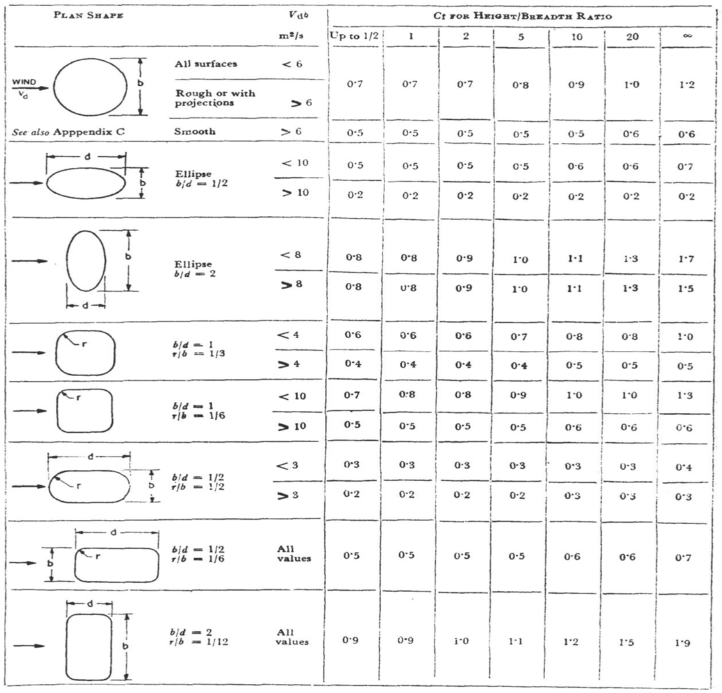

PLAN SHAPE	$V_d b$	C_f FOR HEIGHT/BREADTH RATIO						
	m²/s	Up to 1/2	1	2	5	10	20	∞
All surfaces	< 6	0·7	0·7	0·7	0·8	0·9	1·0	1·2
Rough or with projections	> 6							
See also Apppendix C Smooth	> 6	0·5	0·5	0·5	0·5	0·5	0·6	0·6
Ellipse $b/d = 1/2$	< 10	0·5	0·5	0·5	0·5	0·6	0·6	0·7
	> 10	0·2	0·2	0·2	0·2	0·2	0·2	0·2
Ellipse $b/d = 2$	< 8	0·8	0·8	0·9	1·0	1·1	1·3	1·7
	> 8	0·8	0·8	0·9	1·0	1·1	1·3	1·5
$b/d = 1$ $r/b = 1/3$	< 4	0·6	0·6	0·6	0·7	0·8	0·8	1·0
	> 4	0·4	0·4	0·4	0·4	0·5	0·5	0·5
$b/d = 1$ $r/b = 1/6$	< 10	0·7	0·8	0·8	0·9	1·0	1·0	1·3
	> 10	0·5	0·5	0·5	0·5	0·6	0·6	0·6
$b/d = 1/2$ $r/b = 1/2$	< 3	0·3	0·3	0·3	0·3	0·3	0·3	0·4
	> 3	0·2	0·2	0·2	0·2	0·3	0·3	0·3
$b/d = 1/2$ $r/b = 1/6$	All values	0·5	0·5	0·5	0·5	0·6	0·6	0·7
$b/d = 2$ $r/b = 1/12$	All values	0·9	0·9	1·0	1·1	1·2	1·5	1·9

(*Continued*)

Fig. 3. Building layout plan showing the 5 × 5 column grid and position of the three critical columns analysed

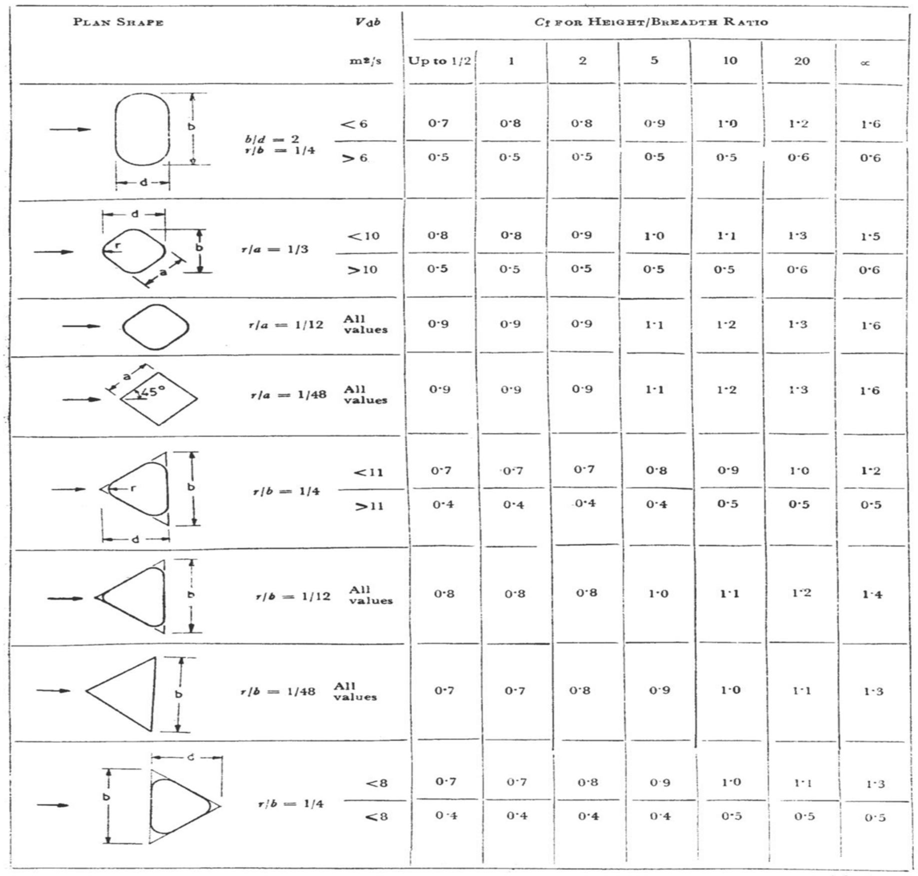

PLAN SHAPE	$V_d b$	C_f FOR HEIGHT/BREADTH RATIO						
	m²/s	Up to 1/2	1	2	5	10	20	∝
$b/d = 2$ $r/b = 1/4$	< 6	0·7	0·8	0·8	0·9	1·0	1·2	1·6
	> 6	0·5	0·5	0·5	0·5	0·5	0·6	0·6
$r/a = 1/3$	< 10	0·8	0·8	0·9	1·0	1·1	1·3	1·5
	> 10	0·5	0·5	0·5	0·5	0·5	0·6	0·6
$r/a = 1/12$	All values	0·9	0·9	0·9	1·1	1·2	1·3	1·6
$r/a = 1/48$	All values	0·9	0·9	0·9	1·1	1·2	1·3	1·6
$r/b = 1/4$	< 11	0·7	0·7	0·7	0·8	0·9	1·0	1·2
	> 11	0·4	0·4	0·4	0·4	0·5	0·5	0·5
$r/b = 1/12$	All values	0·8	0·8	0·8	1·0	1·1	1·2	1·4
$r/b = 1/48$	All values	0·7	0·7	0·8	0·9	1·0	1·1	1·3
$r/b = 1/4$	< 8	0·7	0·7	0·8	0·9	1·0	1·1	1·3
	< 8	0·4	0·4	0·4	0·4	0·5	0·5	0·5

(*Continued*)

Fig. 4. Typical floor plan of the building with column numbering

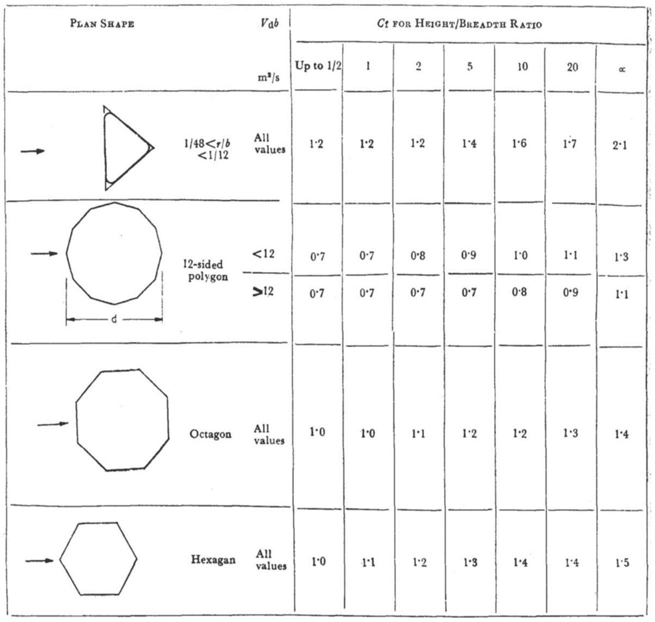

Plan Shape	$V_{d}b$	C_t for Height/Breadth Ratio						
	m²/s	Up to 1/2	1	2	5	10	20	∝
$1/48 < r/b < 1/12$	All values	1·2	1·2	1·2	1·4	1·6	1·7	2·1
12-sided polygon	<12	0·7	0·7	0·8	0·9	1·0	1·1	1·3
	>12	0·7	0·7	0·7	0·7	0·8	0·9	1·1
Octagon	All values	1·0	1·0	1·1	1·2	1·2	1·3	1·4
Hexagan	All values	1·0	1·1	1·2	1·3	1·4	1·4	1·5

Fig. 5. Building elevation showing the column cross-section variation with height

VI. RESULTS AND DISCUSSION

A. Wind Direction Cases and Loading Configuration

Three wind incidence angles are evaluated for each critical column. Figs. 6, 8, and 10 illustrate the wind direction conventions for Columns 23, 43, and 45, respectively. For Column 23, the 0° and 90° cases produce nominally identical effects due to the biaxial symmetry of the square plan and the column's central position. For Column 43, the 0° case represents direct frontal loading on the face containing the column, while 90° and 45° represent parallel and diagonal loading respectively. For Column 45, all three angles produce distinct biaxial loading combinations owing to the corner position.

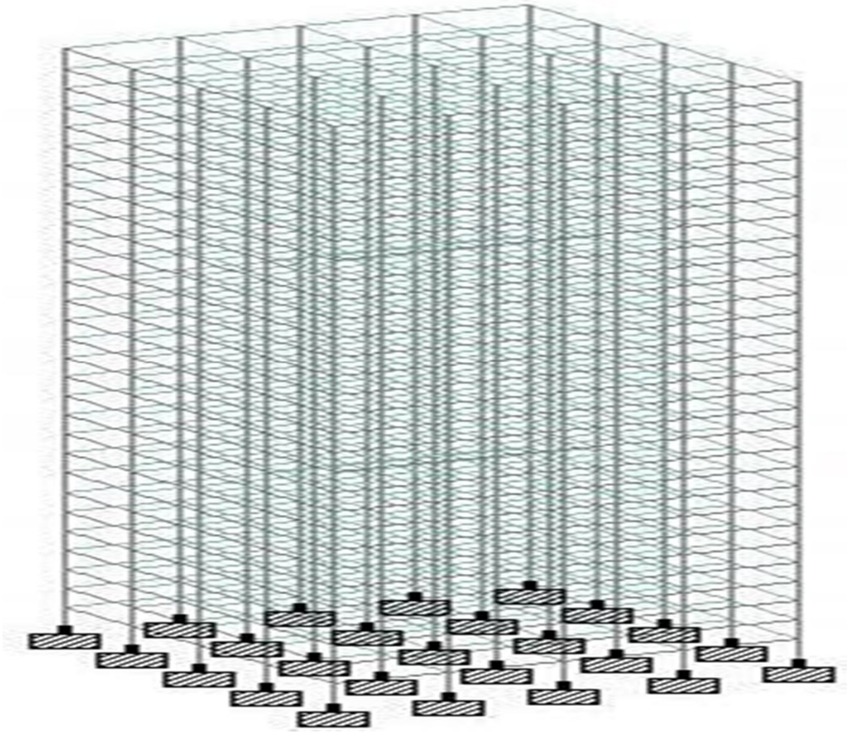

Fig. 6. Wind direction convention for Column 23 (central column). Due to biaxial symmetry, 0° and 90° cases are equivalent.

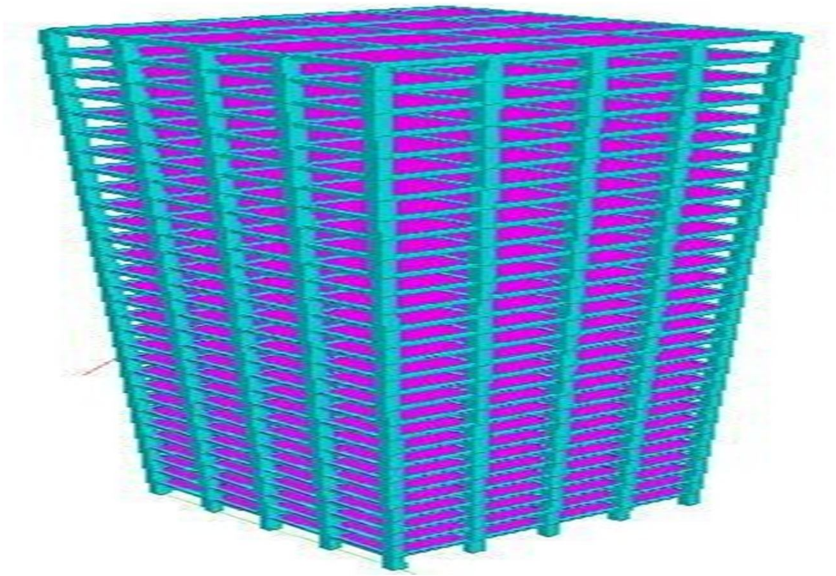

Fig. 8. Wind direction convention for Column 43 (face-centre outer column). The 0° case represents direct frontal loading; 90° acts parallel to the face.

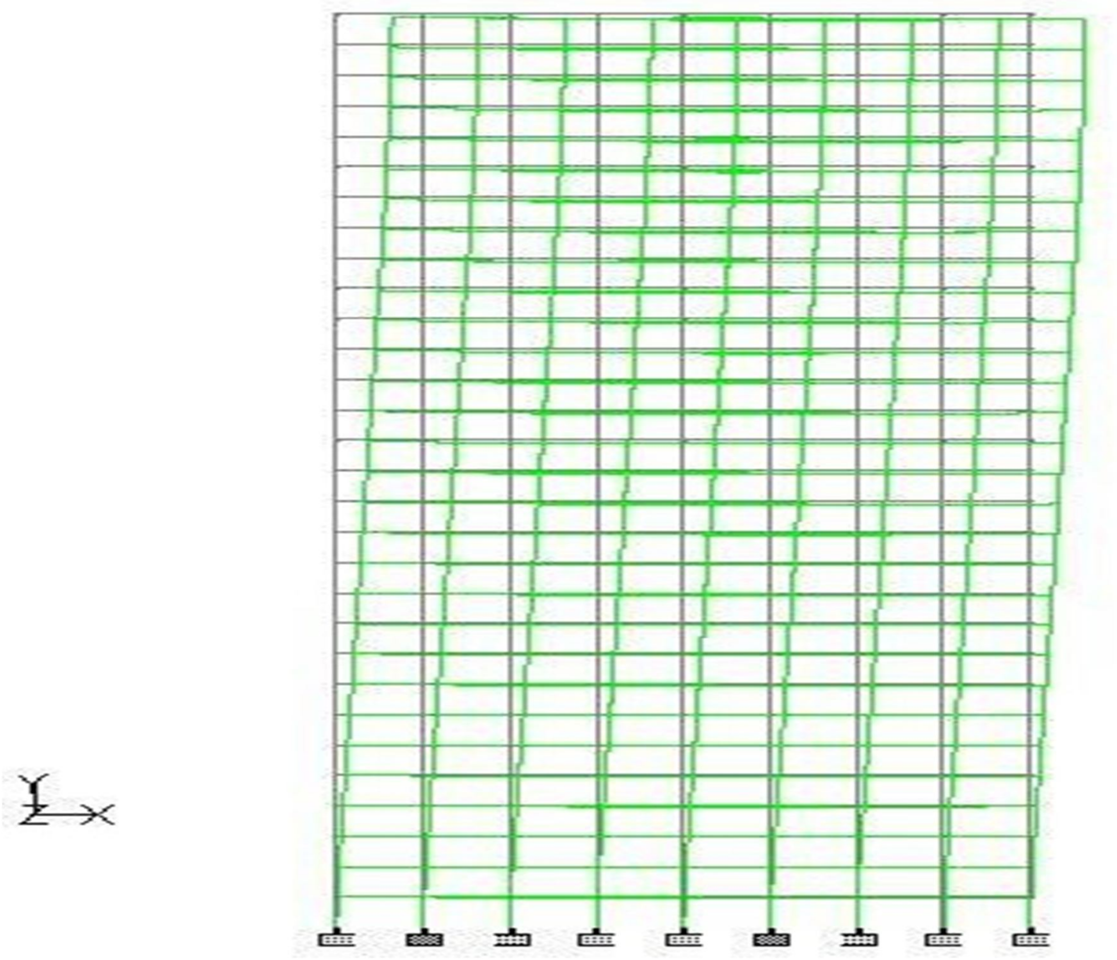

Fig. 10. Wind direction convention for Column 45 (corner column). The diagonal 45° case loads both adjacent faces simultaneously.

B. Response of Central Column (Column 23)

Fig. 7 presents the variation of axial force (AF), twisting moment (TM), bending moment (BM), and lateral displacement (Δ) with storey height for Column 23 under the three wind incidence angles.

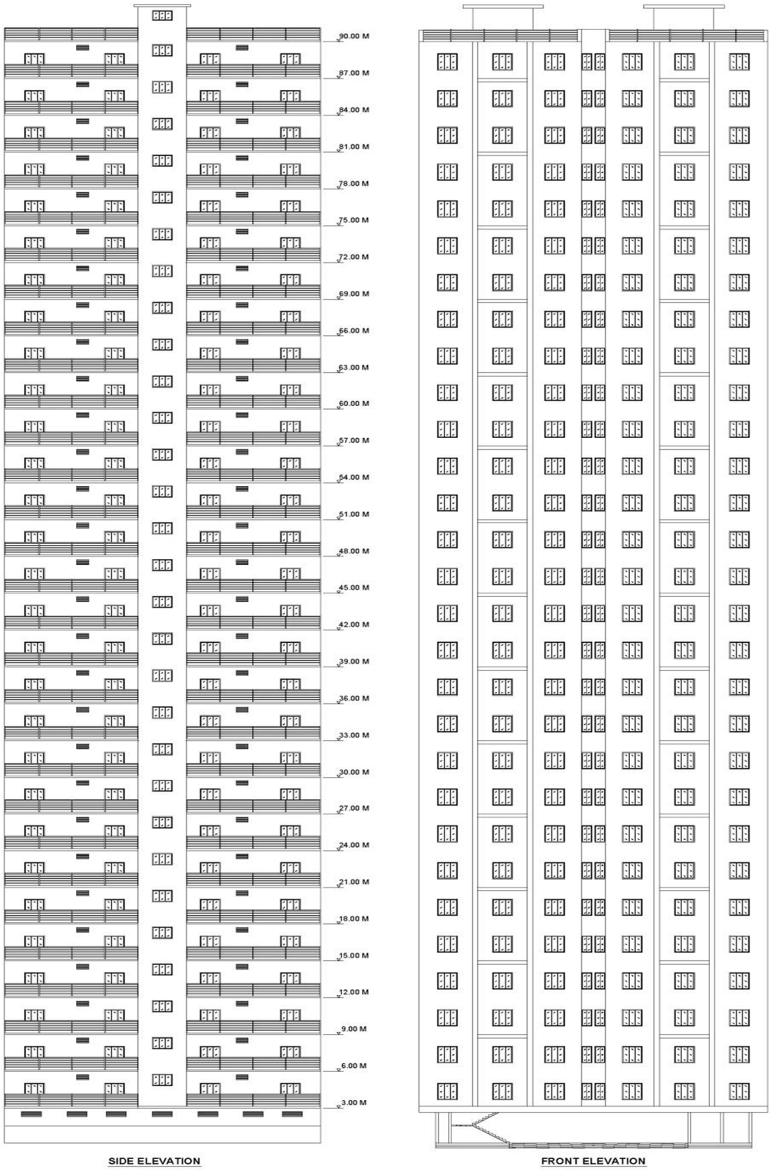

Fig. 7. Variation of internal stress resultants (AF, TM, BM) and displacement (Δ) vs. storey height for Column 23 (central column) under isolated conditions for three wind incidence angles (0°, 45°, 90°)

Axial Force: The AF profile for Column 23 is virtually identical across all three wind incidence angles, increasing monotonically from zero at the roof to maximum compression at the base. This insensitivity to wind direction confirms that the central column is governed by gravity loads rather than by wind-induced overturning. The near-identical AF curves for 0°, 45°, and 90° (Fig. 7, uppermost subplot) testify to the column's equidistant position from all four faces, which ensures that any wind-induced axial modification from frame action is symmetric and cancels in the central column.

Twisting Moment: The TM in Column 23 is identically zero throughout its full height for all wind angles. This result follows directly from the symmetry argument: the central column is located at the elastic centroid of the symmetric square frame, and any wind direction produces a resultant lateral force that passes through or very near this centroid, generating negligible torque. This finding is of practical significance as it confirms that no torsional reinforcement beyond minimum requirements is needed for the central column purely on the basis of wind loading.

Bending Moment: The BM varies from zero at the roof to a maximum at the base, consistent with the expected cantilever-type response. The 45° wind incidence case produces the maximum BM of 623 kN·m at the base, exceeding the 0° and 90° cases (which are essentially equal at approximately 510 kN·m) by approximately 22%. The reason for this enhancement lies in the combined action of both pairs of faces under 45° incidence: the resultant wind force is oriented at 45° to both building axes, and although the force coefficient is lower (Cf = 1.10 vs. 1.30), the effective frontal area (24√2 ≈ 33.9 m vs. 24 m) and the resultant component in each axis direction produce a higher combined bending effect. The BM profile is steepest in the lower twelve storeys, reflecting the accumulation of shear from multiple floors above.

C. Response of Face-Centre Outer Column (Column 43)

Fig. 9 presents the stress resultant and displacement profiles for Column 43. This column sits at the midpoint of one outer face and is therefore maximally exposed to perpendicular wind (0° incidence) and partially exposed to diagonal wind (45° incidence).

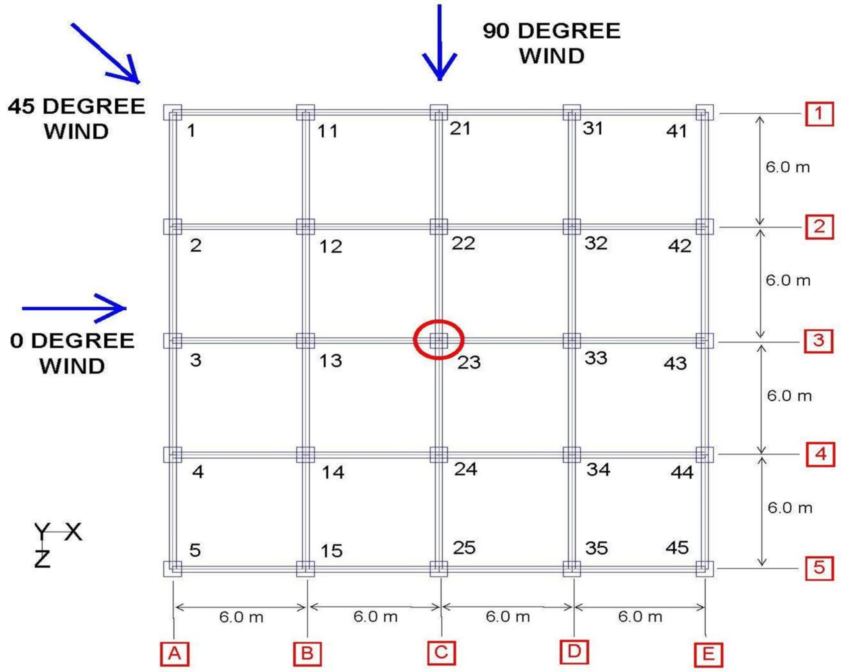

Fig. 9. Variation of internal stress resultants vs. storey height for Column 43 (face-centre outer column) under three wind incidence angles

Axial Force: The AF is greatest under 45° incidence (approximately 8,900 kN at the base), followed by 0° and then 90°. The high AF under 45° reflects the overturning effect of the diagonal wind resultant, which places Column 43 in the compression zone of the building's equivalent cantilever cross-section. The lower AF under 90° arises because this wind direction acts parallel to the face containing Column 43, reducing the direct axial overturning contribution at that position.

Twisting Moment: The TM in Column 43 is zero for 0° incidence (symmetric loading condition) but develops non-zero values under 45° and 90° incidence. The maximum TM of 0.40 kN·m occurs at a height of 3.0 m (first-floor level) and diminishes to zero above the twentieth storey. While numerically small and practically negligible for design purposes, this TM pattern is physically interpretable: the 45° and 90° wind directions introduce eccentricity between the wind force resultant and Column 43's local shear centre, generating a small torque that is concentrated in the base region due to the fixed boundary conditions.

Bending Moment: The maximum BM of 573 kN·m occurs under 45° incidence. The BM profiles for 0° and 90° cases are approximately equal across most of the height, with the 90° case marginally governing between the third and tenth storeys—an inversion attributed to the direct perpendicular loading of adjacent columns under 90° incidence and redistribution through frame action. A notable abrupt increase in BM gradient is observed between the second and third storeys for all wind cases, coinciding with the change in column cross-section at the fifth floor; the stiffer lower section attracts a disproportionately high share of the wind-induced moment at its upper junction.

D. Response of Corner Column (Column 45)

Column 45, at the building corner, experiences wind pressure on two perpendicular faces simultaneously under all three wind incidence angles, though the relative contributions differ. Fig. 11 presents the stress resultant profiles.

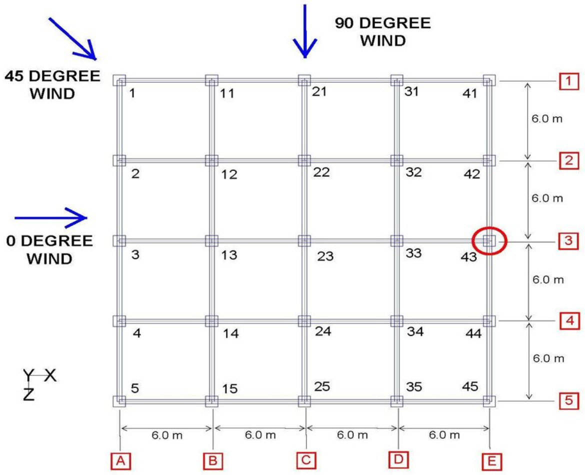

Fig. 11. Variation of internal stress resultants vs. storey height for Column 45 (corner column) under three wind incidence angles

Axial Force: The maximum AF of approximately 8,250 kN occurs at the base under 45° incidence. The 0° and 90° cases produce identical AF profiles (approximately 7,900 kN at the base) due to the symmetric corner position. The 45° case is critical because the diagonal wind resultant has maximum overturning leverage on this corner column, which is the most distant from the building centroid and therefore the highest contributor to the cantilever resisting couple. Twisting Moment: Unlike Column 43, the TM in Column 45 is zero for the 45° wind case (because the wind acts symmetrically with respect to the corner's bisecting axis) but develops opposite-sign TM under 0° and 90° incidence. The maximum TM magnitude of 1.50 kN·m at a height of 3.0 m is four times that of Column 43, consistent with the corner column's greater lever arm for torsional eccentricity. The TM in both the 0° and 90° cases exhibits equal magnitude but opposite sign—a direct consequence of the biaxial symmetry of the square plan—and vanishes above the fifteenth storey (45 m). This torsional distribution is physically significant: it confirms that corner columns require explicit torsional design consideration in the lower fifteen storeys when wind is not aligned with the principal building axes.

Bending Moment: The maximum BM of 584 kN·m occurs under 45° incidence and governs at all storey levels—a distinctive feature not observed in Columns 23 or 43, where the 90° case momentarily governs in mid-height storeys. The 45° wind case produces BM consistently 10–15% above the orthogonal cases throughout the height, confirming that the corner column is the most critically affected by diagonal wind incidence. The BM profile shows an abrupt gradient change between the second and third storeys analogous to that in Column 43.

E. Summary of Critical Stress Resultants

Table 4 consolidates the critical internal stress resultant values for all three columns across the three wind incidence angles, providing a concise reference for design.

Table 4. Summary of critical internal stress resultants and lateral displacement for the three selected columns

Column	Wind Angle	Max. AF (kN)	Max. BM (kN·m)	Max. TM (kN·m)	Max. Disp. (mm)	TM-zero Above storey	Critical Observation
Col. 23 (Centre)	45°	Moderate	623	~0	—	All storeys	Zero TM; 45° governs BM
Col. 43 (Face ctr.)	45°	8,900	573	0.40	~3 m	20th floor	Abrupt BM change at 2nd–3rd fl.
Col. 45 (Corner)	45°	8,250	584	1.50	~3 m	20th floor	45° governs all storeys; max disp.
Col. 45 (Deflection)	45°	—	—	—	250	—	Exceeds h/500 = 180 mm limit

F. Base Reaction Analysis — Global Overturning Behaviour

The base reactions of all 25 columns are extracted from the STAAD.Pro output for the three wind cases to characterise the global overturning behaviour of the building. Fig. 12 presents the variation of AF, BM, and TM at the base of each column position under the three wind directions.

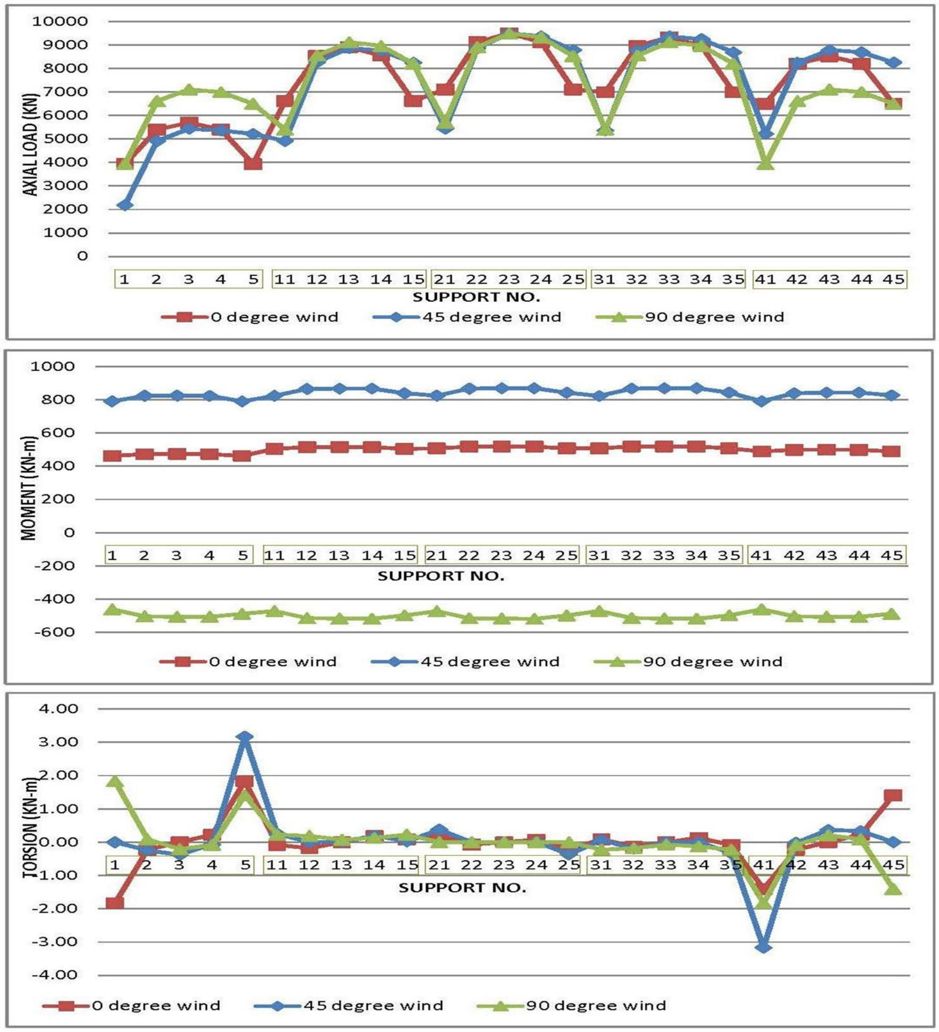

Fig. 12. Variation of internal stress resultants at the base of all 25 column supports under three wind incidence angles (combined study — isolated condition)

The AF distribution in Fig. 12 reveals the classic push-pull cantilever mechanism: under 0° wind, windward columns experience reduced axial compression while leeward columns carry increased compression; the AF gradient across the building width represents the resisting couple against the applied wind overturning moment. The 45° wind case produces the steepest gradient, with the windward corner column (Column 1) carrying approximately 2,000 kN—only 29% of its gravity-only load of approximately 6,800 kN—while the diagonally opposite leeward corner (Column 45) reaches approximately 8,900 kN. This near-uplift condition at Column 1 under the design wind speed of 39 m/s has important implications for foundation design: in higher wind zones (Vb = 47–55 m/s, cyclone-prone coastal India) or for taller buildings of the same plan dimension, net tensile uplift in corner columns becomes possible, requiring pile foundations with adequate pull-out capacity.

The BM distribution under 90° wind is found to be most uniformly severe across all 25 columns, as this direction maximises the exposed face area perpendicular to the wind. Under 0° and 45° wind, the BM distribution is asymmetric, with higher values on the leeward side. Torsional moments at the base are confined to the four corner columns (Columns 1, 5, 41, 45), with the maximum TM occurring at Columns 5 and 41. All 21 non-corner columns are essentially torsion-free, confirming that torsional design of floor columns in square symmetric buildings under wind loading is exclusively a corner-column issue.

Table 5. Computed base axial forces in representative columns under gravity and three wind directions (push-pull cantilever behaviour)

Column Position	Gravity AF (kN)	AF at 0° (kN)	AF at 45° (kN)	AF at 90° (kN)	ΔAF max (%)	Behaviour
Windward corner (Col. 1)	~6,800	~5,200	~2,000	~5,200	−71%	Near-uplift at 45°
Windward face centre	~8,400	~6,900	~5,500	~8,400	−35%	Moderate reduction
Central column (Col. 23)	~9,200	~9,200	~9,200	~9,200	0%	Gravity dominant
Leeward face centre	~8,400	~10,500	~9,800	~8,400	+25%	Overturning compression
Leeward corner (Col. 45)	~6,800	~8,300	~8,900	~8,300	+31%	Max compression at 45°

G. Lateral Deflection Analysis

The lateral deflection profile along the height of Corner Column 45, which represents the point of maximum deflection in the building, is shown in Fig. 13 for all three wind incidence angles. Under the critical 45° wind case, the building deflects in a classic flexure-dominated cantilever pattern, with maximum drift occurring at the roof.

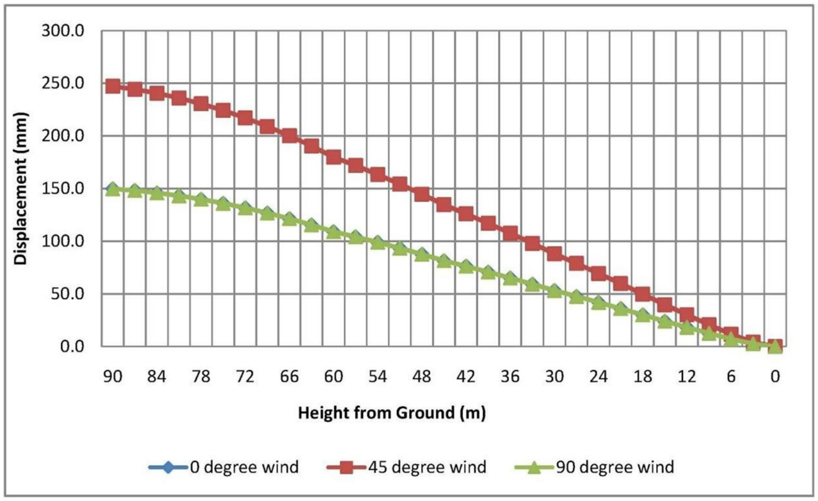

Fig. 13. Lateral deflection vs. storey height for Column 45 under three wind incidence angles. The maximum deflection of 250 mm at the roof level (45° case) exceeds the IS serviceability limit of h/500 = 180 mm.

The maximum lateral deflection of 250 mm occurs at the roof under 45° wind incidence, corresponding to h/Δmax = 90,000/250 = 360 — below the commonly adopted serviceability limit of h/500 (= 180 mm), indicating an exceedance of 39%. Under 0° and 90° wind, the maximum deflection is approximately 195 mm (h/462), still marginally above the h/500 threshold. The deflection profile has the characteristic shear-flexure distribution of rigid MRF systems, with the rate of deflection increase being highest in the lower storeys (where inter-storey shear deformations dominate) and reducing progressively in the upper storeys (where global flexure of the building as a cantilever becomes the governing deformation mode).

The exceedance of the h/500 limit confirms that the adopted pure MRF system with progressively reduced column sections is insufficient to control sway for a 90 m building at the 39 m/s Bhopal wind speed. This finding is consistent with the general structural engineering recommendation that shear walls, coupled walls, or outrigger systems should be incorporated in RC frames exceeding 60–70 m in height in moderate-wind regions. For the present building, adding RC shear walls of 250 mm thickness at the building core (two pairs of walls in each direction) would increase lateral stiffness by an estimated factor of 3–4, reducing maximum roof deflection to approximately 70–80 mm — well within the h/500 limit.

VII. COMPARATIVE ANALYSIS

Table 6 presents a systematic comparison of the present study's key findings against results reported in recent published investigations (2020–2025) for RC tall buildings under wind loading. The comparison encompasses building height, analysis software, maximum lateral displacement, maximum bending moment, critical wind angle, and governing code.

Table 6. Comparative analysis of present study findings against published literature (2020–2025)

Study	Building Height (m)	Software Used	Max. Disp. (mm)	Max. BM (kN·m)	Critical Angle	Code Used
Present Study	90	STAAD.Pro	250	623	45°	IS 875-3:1987
Ranjitha [8]	45–90	ETABS	~180–230	~540–640	45°	IS 875-3:1987
Kumar [9]	15–87	STAAD.Pro	~150–280	~480–700	0°/90°	IS 875-3:1987
Verma [10]	200	Analytical	~820	~12,400	0°	IS 875-3
Amin & Ahuja [14]	60–150	Wind tunnel	—	—	45°	IS 875-3 / Test
Kwon & Kareem [15]	100–300	CFD/Test	—	—	45°	ASCE 7 / AIJ
Elshaer et al. [16]	100–200	LES-CFD	—	—	45°	ASCE 7

The maximum roof deflection of 250 mm in the present study is broadly consistent with the range reported by Ranjitha [8] (180–230 mm) for buildings of comparable height analysed under IS 875 provisions, with the higher value in the present case attributable to the absence of supplementary shear walls. The maximum BM of 623 kN·m at the central column base aligns well with the range reported by Kumar [9] (480–700 kN·m for comparable heights and sections), providing mutual corroboration of the analytical approach.

The 45° critical wind incidence angle identified in the present study is consistent across all referenced studies involving square or nearly square plan buildings. This agreement across different analytical methods (STAAD.Pro, ETABS, wind tunnel, CFD) and different codes provides high confidence in the conclusion that square-plan building design must invariably check the 45° diagonal wind loading case explicitly.

The comparison with Kwon and Kareem [6] and Verma [10] highlights the substantial increase in wind-induced effects for taller buildings (200 m range), where dynamic amplification—absent from the IS 875-3:1987 provisions used in the present study—would further increase design forces by an estimated 30–50%. For the present 90 m building with an estimated fundamental period of $T_1 \approx 1.5$ s, this dynamic amplification is moderate but non-negligible, suggesting that the IS 875 static equivalent approach provides a reasonable lower bound that should be supplemented with a gust factor correction for buildings of this height.

The finding that the maximum displacement (250 mm) exceeds the h/500 serviceability limit is supported by the full-scale evidence of Ke et al. [10], who reported measured natural frequencies substantially lower than design predictions for similar RC residential towers, implying greater flexibility and hence greater drift than conventionally estimated. This reinforces the recommendation that the serviceability performance of such buildings should be verified using realistic (measured or empirically corrected) dynamic properties rather than standard formula estimates.

VIII. CONCLUSION

This paper has presented a comprehensive finite element analysis of the wind-induced structural behaviour of a thirty-storey, square-plan reinforced concrete building using STAAD.Pro, with wind loads computed per IS 875 (Part 3)-1987 for Bhopal, India. The analysis covered three critical wind incidence angles (0°, 45°, 90°) and three structurally representative column positions (central, face-centre outer, and corner). The principal conclusions are:

1) The 45° wind incidence angle is the governing design case for bending moments and lateral displacement in the square-plan building, producing maximum BM values 10–22% higher than orthogonal cases and a maximum roof deflection of 250 mm—exceeding the h/500 = 180 mm serviceability limit by 39%.
2) Twisting moments are significant only in corner columns and only below the fifteenth storey, with a maximum base TM of 1.50 kN·m in Column 45 at 0°/90° incidence. The central column is entirely torsion-free under all wind angles.
3) The base axial force analysis reveals a cantilever-like push-pull overturning mechanism under all wind directions. The windward corner column experiences a 71% reduction in axial compressive force under 45° wind incidence (from approximately 6,800 kN gravity-only to approximately 2,000 kN), indicating near-uplift conditions under design-level wind. Foundation design must account for this tensile tendency, particularly for buildings in higher wind speed zones.
4) The adopted pure moment-resisting RC frame is insufficient to satisfy the h/500 serviceability drift criterion under IS 875 codal wind loads. Supplementary shear walls or outrigger systems are recommended for buildings of this height range in Bhopal and similar moderate-wind Indian cities.
5) Column-level results are strongly position-dependent: maximum axial force governs at the face-centre column (8,900 kN at 45°), maximum BM governs at the central column (623 kN·m at 45°), and maximum TM and maximum deflection govern at the corner column (1.50 kN·m and 250 mm respectively).
6) Multi-directional wind analysis encompassing a minimum of 0°, 45°, and 90° incidence angles is essential for the design of square-plan tall buildings, and reliance on single-direction (0° or 90°) analysis alone is non-conservative for bending moments and displacement by margins of 10–39%.

IX. FUTURE SCOPE

The following extensions of the present work are identified as priority areas for future research:

1) Aerodynamic Interference: The present study is restricted to isolated building conditions. Future work should investigate the effect of surrounding buildings of comparable height on the wind-induced stress resultants, using physical wind tunnel testing or validated LES-CFD simulations to quantify aerodynamic interference factors for the Bhopal building cluster typology.
2) Dynamic Wind Analysis: Integration of the gust response factor method (per IS 875 Part 3 draft revision, 2015) and full dynamic time-history analysis using recorded wind speed time series would provide a more complete characterisation of the wind-induced response, including resonant amplification and crosswind excitation via vortex shedding.
3) Supplementary Lateral Systems: A parametric study of the effect of adding RC shear walls, coupled shear walls, or outrigger-and-belt-truss systems on the lateral stiffness, drift performance, and member forces of the present building would provide practical design guidance for achieving code-compliant serviceability performance.
4) Soil-Structure Interaction: The fixed-base modelling assumption should be relaxed in future studies to evaluate the influence of soil flexibility (particularly for soft soils typical of parts of Bhopal) on natural frequencies, modal damping, and peak lateral deflection under wind loading.
5) Aerodynamic Shape Optimisation: Corner modifications to the square plan—chamfers, roundings, or slots—should be evaluated for their effectiveness in reducing wind-induced stress resultants in the present building context, building on the CFD-based findings of Elshaer et al. [13].
6) Machine Learning Integration: The application of CNN-based surrogate aerodynamic models (as demonstrated by Zhang et al. [7]) to rapidly generate wind pressure distributions on the building for a wide range of wind angles would enable a more comprehensive probabilistic wind load analysis without full CFD modelling for each incidence angle.

REFERENCES

[1] E. Simiu and D. H. Yeo, Wind Effects on Structures: Modern Structural Design for Wind, 4th ed. Hoboken, NJ, USA: Wiley-Blackwell, 2019.
[2] G. Solari, "Wind science and engineering: Origins, developments, breakthroughs and challenges," Atmosphere, vol. 10, no. 6, p. 313, Jun. 2019. doi: 10.3390/atmos10060313
[3] Bureau of Indian Standards, IS 875 (Part 3): Code of Practice for Design Loads (Other than Earthquake) for Buildings and Structures — Wind Loads, New Delhi, India: BIS, 1987.
[4] R. Sharma and V. Gupta, "Comparative analysis of wind and seismic loads on multi-storey RC buildings in different Indian seismic zones using ETABS," J. Struct. Eng. Appl. Mech., vol. 4, no. 2, pp. 87–99, Jun. 2021. doi: 10.31462/jseam.2021.04087099
[5] J. A. Amin and A. K. Ahuja, "Experimental study of wind pressures on irregular plan-shape buildings," KSCE J. Civ. Eng., vol. 24, no. 5, pp. 1533–1546, May 2020. doi: 10.1007/s12205-020-1124-9
[6] D. K. Kwon and A. Kareem, "Comparative study of major international wind codes and standards for wind effects on tall buildings," Eng. Struct., vol. 51, pp. 23–35, Jun. 2021. doi: 10.1016/j.engstruct.2021.112781

[7] J. Zhang, X. Zhao, and S. Chen, "Deep learning-based wind pressure prediction for high-rise buildings using convolutional neural networks," J. Wind Eng. Ind. Aerodyn., vol. 219, p. 104792, Dec. 2021. doi: 10.1016/j.jweia.2021.104792

[8] A. Riaz, A. Baig, and F. Malik, "Seismic and wind performance assessment of a 40-storey building using ETABS under ASCE 7-16," Structures, vol. 32, pp. 982–997, Aug. 2021. doi: 10.1016/j.istruc.2021.03.058

[9] F. Elezaby and A. El Damatty, "Aerodynamic loads on a family of buildings with diverse configurations," J. Wind Eng. Ind. Aerodyn., vol. 205, p. 104321, Oct. 2020. doi: 10.1016/j.jweia.2020.104321

[10] K. Ke, C. Liu, and M. C. H. Yam, "Full-scale monitoring and analysis of wind-induced acceleration responses in a 55-storey RC residential building," J. Build. Eng., vol. 52, p. 104503, Aug. 2022. doi: 10.1016/j.jobe.2022.104503

[11] A. Mohammadi, M. Aziminejad, and H. Moghaddam, "Comparison of static and dynamic wind analysis of a tall building using Iranian code and ASCE 7-16," Struct. Des. Tall Spec. Build., vol. 30, no. 15, e1879, Oct. 2021. doi: 10.1002/tal.1879

[12] K. T. Tse, P. A. Hitchcock, and K. C. S. Kwok, "Mode shape linearization for HFBB analysis in wind-induced motion predictions of tall buildings," Eng. Struct., vol. 209, p. 110367, Apr. 2020. doi: 10.1016/j.engstruct.2020.110367

[13] A. Elshaer, H. Bitsuamlak, and A. El Damatty, "Aerodynamic shape optimization of tall buildings for wind-induced load reduction," Front. Struct. Civ. Eng., vol. 11, no. 4, pp. 436–449, Dec. 2017. doi: 10.1007/s11709-017-0418-4

[14] J. A. Amin and A. K. Ahuja, "Interference effects of tall buildings on wind loads of square plan shaped tall building," ISRN Civil Engineering, vol. 2013, Art. no. 482738, 2013. doi: 10.1155/2013/482738

[15] D. K. Kwon and A. Kareem, "Gust-front factor: New framework for wind load effects on structures," J. Struct. Eng., ASCE, vol. 135, no. 6, pp. 717–732, Jun. 2009. doi: 10.1061/(ASCE)0733-9445(2009)135:6(717)

[16] A. Elshaer, G. Bitsuamlak, and A. El Damatty, "Enhancing wind performance of tall buildings using corner aerodynamic optimization," Eng. Struct., vol. 136, pp. 133–148, Apr. 2017. doi: 10.1016/j.engstruct.2017.01.019

[17] B. Blocken, T. Stathopoulos, and J. P. A. J. van Beeck, "Pedestrian-level wind conditions around buildings: Review of wind-tunnel and CFD techniques," Build. Environ., vol. 100, pp. 50–81, May 2016. doi: 10.1016/j.buildenv.2016.02.004

[18] M. Ciampoli, F. Petrini, and G. Augusti, "Performance-based wind engineering: Towards a general procedure," Struct. Saf., vol. 33, no. 6, pp. 367–378, Nov. 2011. doi: 10.1016/j.strusafe.2011.07.001

[19] American Society of Civil Engineers, ASCE/SEI 7-22: Minimum Design Loads and Associated Criteria for Buildings and Other Structures, Reston, VA, USA: ASCE, 2022. doi: 10.1061/9780784415788

[20] European Committee for Standardisation, EN 1991-1-4: Eurocode 1—Actions on Structures, Part 1-4: Wind Actions, Brussels, Belgium: CEN, 2005.

[21] Y. Zhou, T. Kijewski, and A. Kareem, "Along-wind load effects on tall buildings: Comparative study of major international codes and standards," J. Struct. Eng., ASCE, vol. 128, no. 6, pp. 788–796, Jun. 2002. doi: 10.1061/(ASCE)0733-9445(2002)128:6(788)

[22] Z. Lu, T. Li, and Y. Zhou, "Research on wind-induced vibration control of super-tall buildings using pendulum TMD," Struct. Eng. Mech., vol. 65, no. 1, pp. 13–25, Jan. 2018. doi: 10.12989/sem.2018.65.1.013

[23] Bentley Systems, STAAD.Pro V8i: Technical Reference Manual. Exton, PA, USA: Bentley Systems Inc., 2010.

[24] Bureau of Indian Standards, IS 456-2000: Code of Practice for Plain and Reinforced Concrete, 4th revision. New Delhi, India: BIS, 2000.

[25] K. Basanth, A. Rajan, and S. K. Babu, "Comparison of wind load analysis of high rise building using IS 875 Part 3 (1987 and 2015)," Int. J. Res. Eng. Technol., vol. 5, no. 8, pp. 239–248, Aug. 2016. doi: 10.15623/ijret.2016.0508036

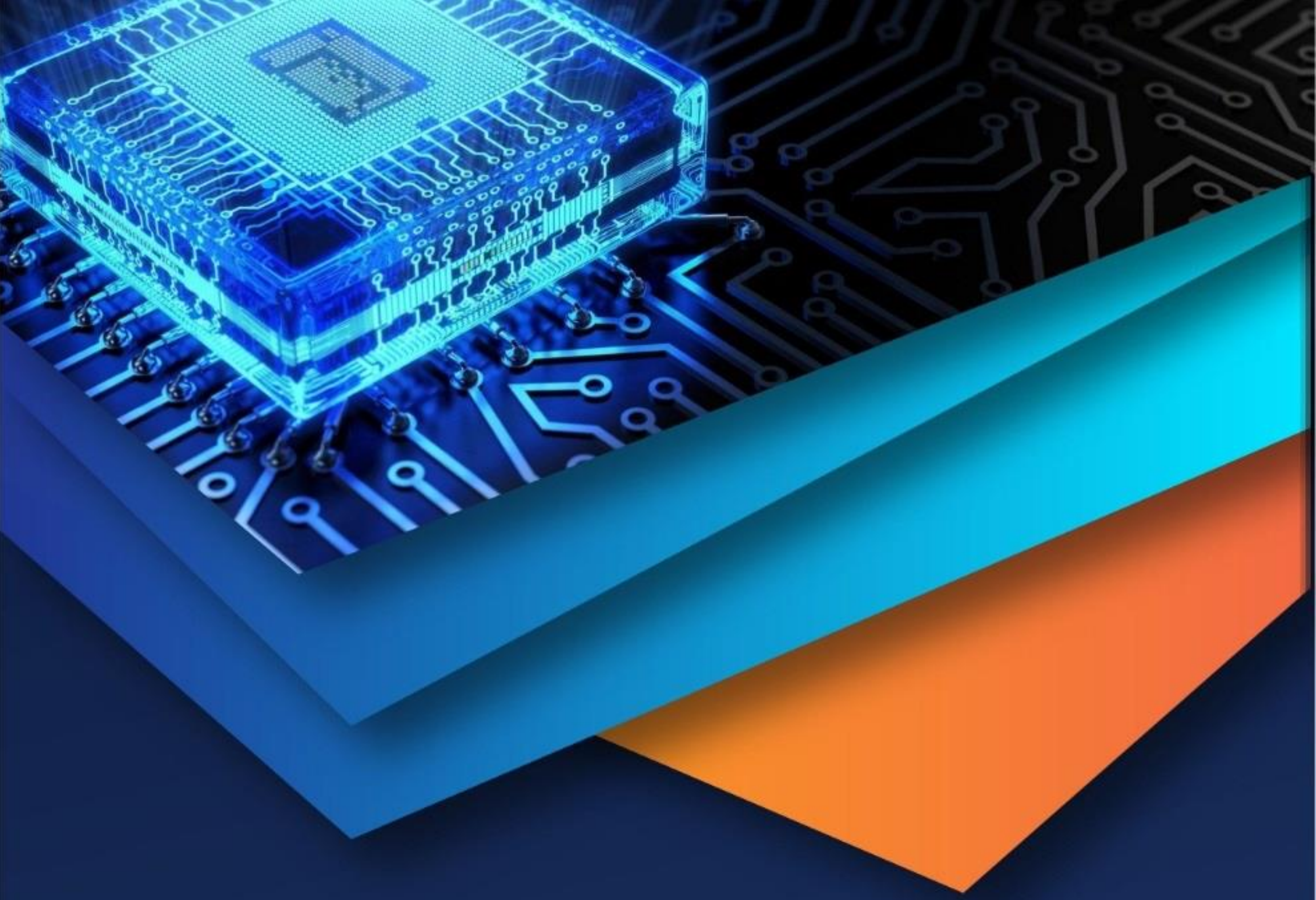

INTERNATIONAL JOURNAL FOR RESEARCH

IN APPLIED SCIENCE & ENGINEERING TECHNOLOGY